

Magnetic dissipation: Spatial and temporal structure

ÅKE NORDLUND

*Niels Bohr Institute and Theoretical Astrophysics Center,
Juliane Maries Vej 30, DK-2100 Copenhagen Ø, Denmark*
aake@astro.ku.dk

Abstract

A magnetically dominated plasma driven by motions on boundaries at which magnetic field lines are anchored is forced to dissipate the work being done upon it, no matter how small the electrical resistivity. Numerical experiments have clarified the mechanisms through which balance between the boundary work and the dissipation in the interior is obtained. Dissipation is achieved through the formation of a hierarchy of electrical current sheets, which appear as a result of the topological interlocking of individual strands of magnetic field. The probability distribution function of the local winding of magnetic field lines is nearly Gaussian, with a width of the order unity. The dissipation is highly irregular in space as well as in time, but the average level of dissipation is well described by a scaling law that is independent of the electrical resistivity.

If the boundary driving is suspended for a period of time the magnetic dissipation rapidly drops to insignificant levels, leaving the magnetic field in a nearly force-free, yet spatially complex state, with significant amounts of free magnetic energy but no dissipating current sheets. Renewed boundary driving leads to a quick return to dissipation levels compatible with the rate of boundary work, with dissipation starting much more rapidly than when starting from idealized initial conditions with a uniform magnetic field.

Application of these concepts to modeling of the solar corona leads to scaling predictions in agreement with scaling laws obtained empirically; the dissipation scales with the inverse square of the loop length, and is proportional to the surface magnetic flux. The ultimate source of the coronal heating is the photospheric velocity field, which causes braiding and reconnection of magnetic field lines in the corona. Realistic, three-dimensional numerical models predict emission measures, coronal structures, and heating rates compatible with observations.

*When driv'n by extreme agitation,
I am subject to fierce dissipation;
In each current sheet
There's created much heat,
And my field thus achieves saturation.*

1. Introduction

Magnetic fields are ubiquitous in astrophysical objects; circumstances where there is no magnetic field present are exceptions. Indeed, much of the non-thermal activity that is observed in astrophysical systems is probably related to the presence of magnetic fields.

Gravity is, indirectly, a major reason for the ubiquitous magnetic activity, because it tends to separate matter into dense and tenuous regions. Magnetic fields that connect such regions are subjected to stress in the dense regions, and are forced to dissipate in the tenuous regions. There, the magnetic field energy density can be many times higher than the thermal and kinetic energy density of the gas, and minor readjustments of the magnetic field may correspond to significant heating and acceleration of the gas.

Understanding the principles that control the dissipation of magnetic energy when the plasma beta ($\beta = P_g/P_B$, where P_g is gas pressure and P_B is magnetic pressure) is low and the magnetic Reynolds number ($R_m = UL/\eta$, where U is velocity, L size, and η magnetic diffusivity) is very high is a major challenge, and numerous research papers, review articles and books have been published on this subject over the years (e.g., Parker 1972, 1983, 1988, 1994; Sturrock & Uchida 1981; van Ballegooijen 1986; Mikić et al. 1989; Heyvaerts & Priest 1992; Longcope & Sudan 1994; Galsgaard and Nordlund 1996ab; Nordlund & Galsgaard 1997; Gomez, Dmitruk & Milano 2000; to mention just a few).

The solar corona is an ideal ‘test site’ for theories and models of magnetic dissipation, since it provides rich opportunities for observing both the spatial and temporal structure of a dissipating low beta plasma. The Sun is indeed a ‘Rosetta stone’ in the context of magnetic dissipation—once we understand how magnetic dissipation occurs under such well observed conditions we may be much more confident when extrapolating to more distant and less well observed circumstances.

Numerical experiments have emerged as a complementary and rich source of inspiration in the quest to understand magnetic dissipation. Below I briefly summarize conclusions from two types of experiments; generic experiments where a low beta plasma is driven from two opposing boundaries, and realistic experiments that attempt to model solar coronal conditions as closely as possible.

2. Boundary driven magnetic dissipation

Generic experiments demonstrate that magnetic dissipation does not occur in simple, monolithic current sheets, even if the boundary motions are large scale and slow (cf. Galsgaard and Nordlund 1996a for details

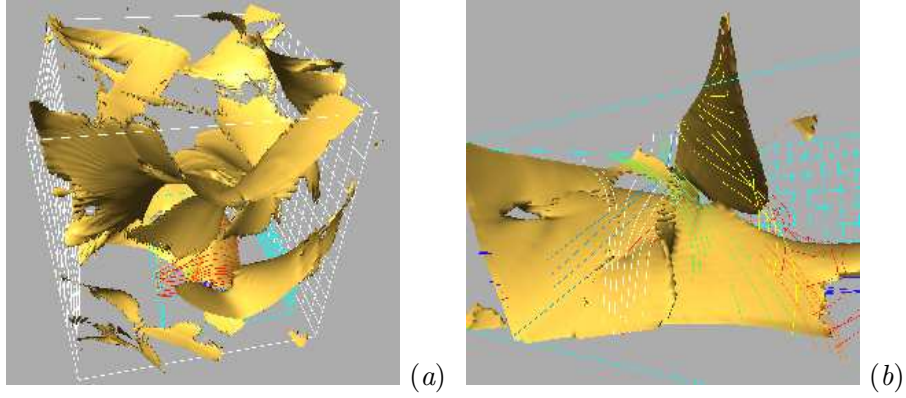


Figure 1. a) Hierarchy of current sheets, shown as isosurfaces of constant electric current density (Galsgaard and Nordlund 1996a). b) Detail of the hierarchy.

about such experiments). Rather, a hierarchy of current sheets form, with smaller scale current sheets protruding from larger scale ones (cf. Fig. 1).

On the average, the collective dissipation in the hierarchy of current sheets balances the boundary work, as it must, to satisfy energy conservation. The average level of work and dissipation at which the equilibrium is obtained does not depend noticeably on the resistivity (or, equivalently, the numerical resolution), as long as the magnetic Reynolds number is not too small. The work W , and hence the dissipation Q times the distance L between the boundaries, is proportional to the energy density of the magnetic field at the boundary, the average angle of inclination ϕ of the magnetic field at the boundary, and the boundary velocity v_b .

$$W_b = QL \sim \frac{B^2}{8\pi} \tan \phi v_b \quad (1)$$

The crucial angle factor $\tan \phi$ scales as $\tan \phi \sim v_b \tau_b / L \sim \ell_b / L$, where τ_b is the autocorrelation time of the boundary motions, ℓ_b is the “stroke length” of the boundary motions, and L is the distance between the driving boundaries. The average dissipation thus scales as

$$Q \sim \frac{B^2}{8\pi} \frac{v_b \ell_b}{L^2} \quad (2)$$

(Fig. 2a). Incidentally, it turns out that the scaling of the photospheric motions that drive the solar corona is such that $v_b(\ell_b) \sim 1/\ell_b$, which implies that similar contributions to the driving are obtained from an extended range of scales.

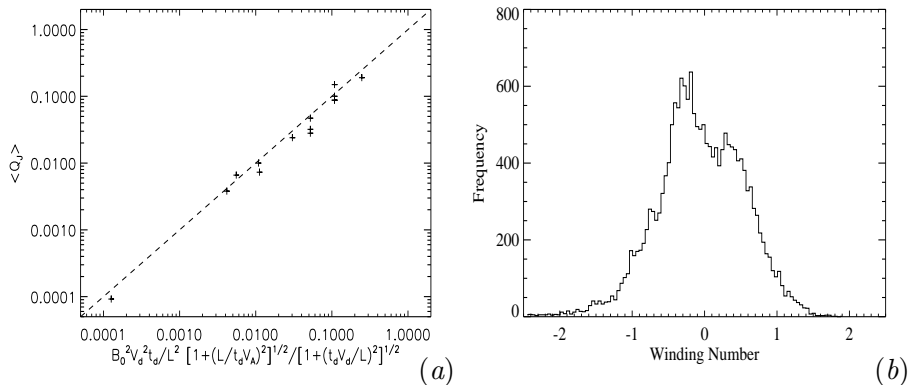


Figure 2. a) Scaling law for magnetic dissipation (Galsgaard and Nordlund 1996a). b) Distribution of winding numbers (Nordlund & Galsgaard 1997).

A sequence of uncorrelated strokes at the two opposing boundaries would, if the connectivity between the boundaries was conserved, lead to further increase of the tilt angles. The magnetic field lines would become increasingly tangled, as each new stroke would cause the end points of field lines connected to neighboring points at one boundary to move further apart at the other boundary.

But the development of current sheets prevents connectivity from being conserved, and prevents the build-up of angles much larger than ℓ_b/L . In the hierarchy of current sheets the smaller current sheets provide a dissipation path for the larger ones, down to the smallest current sheets at a few times the resistive scale. An increase of resolution (magnetic Reynolds number) allows even smaller current sheets to form, but does not change the large scale angles noticeably, and hence does not influence the average level of dissipation.

In terms of the winding of one field line around another, the statistical steady state is one where the number of windings from one boundary to the other has an approximately Gaussian distribution, with a Gaussian width of order unity (Fig. 2b). It is indeed a well known result that a twist much larger than unity leads to violent instability (see Galsgaard & Nordlund 1996b and references cited therein).

3. Suspended / resumed boundary driving

If the external work is suspended dissipation quickly drops, as the current sheets die out. Distributed (smooth) currents remain, but these dissipate much more slowly. The system is in an approximately force-free state, similar to the one just before current sheets first turned on.

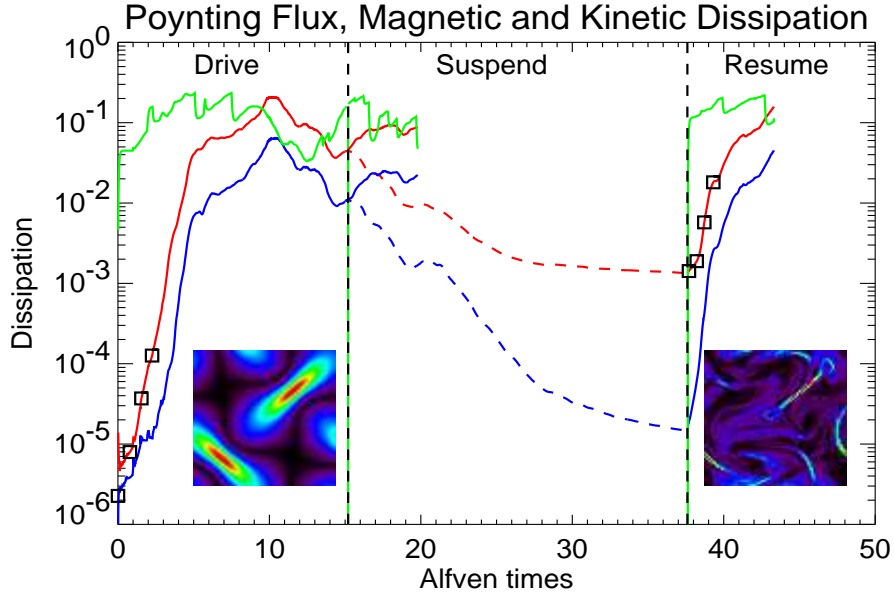


Figure 3. The boundary work (green/top), the magnetic dissipation (red/middle), and the kinetic energy dissipation (blue/lower) in a 3-D numerical experiment (Nordlund and Galsgaard, in preparation) where a magnetically dominated plasma is driven by boundary work at two opposing boundaries. At $t \sim 15$ the boundary work is turned off and the system is allowed to relax until $t \sim 38$, where the initial velocity pattern is repeated again. The two insets show the electric current density in a cross section half-way between the two driving boundaries, approximately two Alfvén crossing times (defined as the length of the box L divided by the Alfvén speed $B/\sqrt{4\pi\rho}$) after the driving has started and resumed, respectively.

When the external work is resumed current sheets return promptly, and dissipation quickly returns to the previous average level (Fig. 3).

Note that, even though exactly the same velocity field is applied for exactly the same time, there are much sharper current concentrations (current sheets) in the right-most inset of Fig. 3, illustrating that the quiescent but spatially complex magnetic field in the suspended state is "ripe" for quickly producing current sheets. The system thus reaches balance between driving and dissipation much more quickly from the suspended driving (\sim force free) state than from the initial (potential) state.

4. Coronal heating experiments

Realistic numerical models of coronal heating and activity are now within reach (Gudiksen & Nordlund 2002), even though the resolution

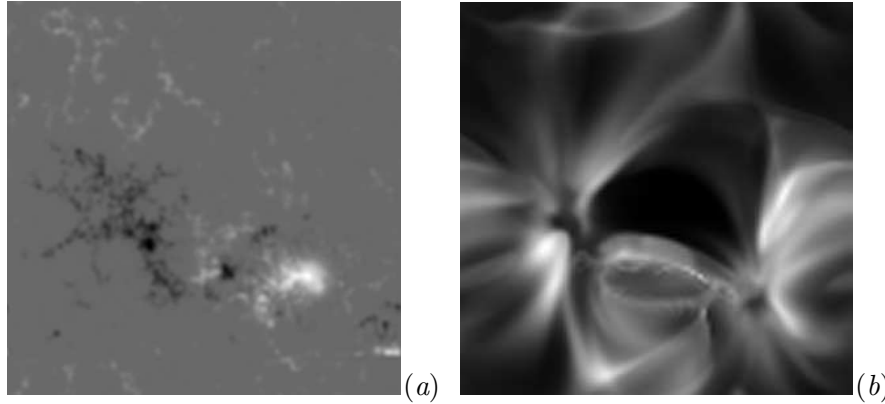


Figure 4. a) The initial condition for the photospheric magnetic field; a high resolution magnetogram of active region 9114, from the Michelson Doppler Interferometer instrument on board the SOHO satellite. b) Synthetic $\lambda 195$ filter image.

constraints are quite severe. In order to apply realistic and well calibrated boundary conditions it is necessary to bridge the distance from the base of the corona to the photospheric surface, where both the magnetic field and the velocity field are known sufficiently well to specify the boundary driving. This limits the vertical resolution to better than, or of the order of, photospheric and chromospheric pressure and density scale heights. The horizontal resolution needs to be similar, to resolve the granular scales where the horizontal velocity amplitudes are largest. The size of a model, on the other hand, needs to be of the order of the size of an active region, or larger. The very high Alfvén velocity in the corona above active regions limits (via the Courant condition) the time step to of the order of 10–30 ms, at the given spatial resolution. Time intervals of at least several granulation turn over times (~ 5 min) need to be covered. The resulting overall constraints are demanding, but not excessively so, given the power of current, massively parallel supercomputers.

With a relevant cooling function approximation (Kahn 1976) and Spitzer conductivity, and by computing synthetic emission measures that correspond closely to those observed from, e.g., the TRACE satellite (Aschwanden, Schrijver & Alexander 2001), one may compare the results directly with solar conditions. With initial conditions taken from a high resolution MDI magnetogram (Fig. 4a), and a random velocity field with scaling properties consistent with a 5 km/s rms solar photospheric velocity field, one obtains average heating rates over an active region $\sim 10^7$ erg cm $^{-2}$ s $^{-1}$, and emission measure images that are similar to observed ones (cf. Fig. 4b).

5. Discussion and concluding remarks

The results of the numerical experiments, and the properties of the scaling law derived from them, provide evidence that we are finally approaching a basic understanding of magnetic dissipation.

First of all, the basic form of the scaling law (2) follows from first principles, and agrees with previously proposed scaling laws (Parker 1983, van Ballegoijen 1986). In addition, it adds a prediction for the crucial inclination factor, for which Parker (1983) and van Ballegoijen (1986) had to make arbitrary assumptions.

Secondly, the scaling law is robust in that the crucial inclination factor is bracketed from above and below. It is bracketed from below because in general current sheets do not develop until the local winding number is of the order of unity. It is bracketed from above, because a local winding number much larger than unity inevitably leads to instabilities that rapidly dissipate the surplus magnetic energy.

Because of the spontaneous formation of a hierarchy of current sheets the scaling law is also robust against changes of the magnetic Reynolds number. If anything, an increased Reynolds number could in principle lead to an *increase* of the magnetic dissipation because, as pointed out by Parker (1988), if one assumes that a reduction of the magnetic diffusivity initially leads to a reduction of the magnetic dissipation the consequence is only that the boundary work for a while exceeds the dissipation, which leads to an increase of the average inclination and hence to a further increase of the boundary work. When the magnetic dissipation eventually comes into balance with the boundary work again it happens at a *higher* level than before.

But in practice, an increase of the magnetic Reynolds number R_m just leads to an extension of the hierarchy of electrical current sheets to smaller scales, which makes it possible to dissipate at the same rate even without increasing the average angle of inclination at the boundaries. Any claim to the contrary must be accompanied by a demonstration that it is possible to sustain a distribution of winding number that is substantially wider than unity at high R_m .

The scaling law (2) is furthermore consistent with scaling laws derived from observations, in that it predicts magnetic dissipation to scale as L^{-2} , in agreement with Porter & Klimchuk (1995). Also, since the solar photosphere has a very intermittent distribution of magnetic field strength B , where B is either very weak or of the order of 1 kG, the average heating is predicted to scale roughly as the magnetic surface filling factor. This again agrees with the observed scaling of coronal heating (Fisher et al. 1998).

Acknowledgments

This work was supported in part by the Danish National Research Foundation through its establishment of the Theoretical Astrophysics Center.

References

- ASCHWANDEN, M. J., SCHRIJVER, C. J. & ALEXANDER, D. 2001 Modeling of Coronal EUV Loops Observed with TRACE. I. Hydrostatic Solutions with Nonuniform Heating. *Astrophysical Journal* **550**, 1036–1050.
- FISHER, G. H., LONGCOPE, D. W., METCALF, T. R. & PEVTSOV, A. A. 1998 Coronal Heating in Active Regions as a Function of Global Magnetic Variables. *Astrophysical Journal* **508**, 885–898.
- GALSGAARD, K. & NORDLUND, Å. 1996a The Heating and Activity of the Solar Corona: I. Boundary Shearing of an Initially Homogeneous Magnetic Field. *Journal of Geophysical Research* **101**, 13445–13460.
- GALSGAARD, K. & NORDLUND, Å. 1996b The Heating and Activity of the Solar Corona: II. Kink Instability in a Flux Tube. *Journal of Geophysical Research* **102**, 219–230.
- GOMEZ, D. O., DMITRUK, P. A. & MILANO, L. J. 2000 Recent theoretical results on coronal heating. *Solar Physics* **195**, 299–318.
- GUDIJKSEN, B. & NORDLUND, Å. 2002 Bulk heating and slender magnetic loops in the solar corona *Astrophys. J. Letters* (submitted)
- HEYVAERTS, J. & PRIEST, E. R. 1992 A self-consistent turbulent model for solar coronal heating *ApJ* **390**, 297–308.
- LONGCOPE, D. W. & SUDAN, R.N. 1994 Evolution and statistics of current sheets in coronal magnetic loops *ApJ* **437**, 491–504.
- MIKIĆ, Z., SCHNACK, D. D., & VAN HOVEN, G. 1989 Creation of current filaments in the solar corona *ApJ* **338**, 1148–1157.
- NORDLUND, Å. & GALSGAARD, K. 1997 Topologically Forced Reconnection. *Lecture Notes in Physics* **489**, 179–200.
- PARKER, E. N. 1972 Topological Dissipation and the Small-Scale Fields in Turbulent Gases. *Astrophysical Journal* **174**, 499–510.
- PARKER, E. N. 1983 Magnetic Neutral Sheets in Evolving Fields. II - Formation of the solar corona. *Astrophysical Journal* **264**, 642–647.
- PARKER, E. N. 1988 Nanoflares and the solar X-ray corona. *Astrophysical Journal* **330**, 474–479.
- PARKER, E. N. 1994 Spontaneous current sheets in magnetic fields: with applications to stellar x-rays. *New York : Oxford University Press, 1994*.
- PORTER, L. J. & KLIMCHUK, J. A. 1995 Soft X-Ray Loops and Coronal Heating. *Astrophysical Journal* **454**, 499–511.
- STURROCK, P. A. & UCHIDA, Y. 1981 Coronal heating by stochastic magnetic pumping *ApJ* **246**, 331
- VAN BALLEGOOLJEN, A. A. 1986 Cascade of magnetic energy as a mechanism of coronal heating *ApJ* **311**, 1001–1014.